DOI:10.1111/j.1477-2574.2011.00409.x HPB

ORIGINAL ARTICLE

Real-time ultrasound imaging of irreversible electroporation in a porcine liver model adequately characterizes the zone of cellular necrosis

Carl R. Schmidt[1], Peter Shires[2] & Mary Mootoo[2]

[1]Department of Surgery, Ohio State University, Columbus, OH, USA and [2]Scientific Affairs Division, Preclinical Department, Ethicon Endo-Surgery, Inc. (a Johnson & Johnson Company), Cincinnati, OH, USA

Abstract

Background: Irreversible electroporation (IRE) is a largely non-thermal method for the ablation of solid tumours. The ability of ultrasound (US) to measure the size of the IRE ablation zone was studied in a porcine liver model.

Methods: Three normal pig livers were treated *in vivo* with a total of 22 ablations using IRE. Ultrasound was used within minutes after ablation and just prior to liver harvest at either 6 h or 24 h after the procedure. The area of cellular necrosis was measured after staining with nitroblue tetrazolium and the percentage of cell death determined by histomorphometry.

Results: Visible changes in the hepatic parenchyma were apparent by US after all 22 ablations using IRE. The mean maximum diameter of the ablation zone measured by US during the procedure was 20.1 ± 2.7 mm. This compared with a mean cellular necrosis zone maximum diameter of 20.3 ± 2.9 mm as measured histologically. The mean percentage of dead cells within the ablation zone was 77% at 6 h and 98% at 24 h after ablation.

Conclusions: Ultrasound is a useful modality for measuring the ablation zone within minutes of applying IRE to normal liver tissue. The area of parenchymal change measured by US correlates with the area of cellular necrosis.

Keywords

irreversible electroporation, ablation, liver neoplasms, ultrasound, surgery, swine

Received 9 June 2011; accepted 10 October 2011

Correspondence

Carl R. Schmidt, Department of Surgery, Ohio State University, Columbus, OH 43054, USA. Tel: + 1 614 293 5644. Fax: + 1 614 366 0003. E-mail: carl.schmidt@osumc.edu

Introduction

Irreversible electroporation (IRE) is a method of causing cell death by applying an electric field across a region of tissue; this results in the permeabilization of cell membranes followed by cellular necrosis.[1] The technique was first described as a method for solid tumour ablation in 2005.[2] The electroporation effect is reversible or irreversible depending on the voltage used, the duration of the electric field and cell membrane fluidity.[3] Electrical pulses lasting microseconds are applied and, with sufficient energy, irreversible permeabilization of the cell membrane occurs, leading to apoptosis.[4] Reversible electroporation has the potential to facilitate DNA transfer for gene therapy or drug delivery in both benign and malignant disease.[5]

Thermal ablation using radiofrequency or microwave energy to treat solid tumours has been applied in several cancers; however, these technologies have some limitations in terms of their efficacy with larger tumours and tumours in proximity to large, intrahepatic vascular structures. The ability to image thermal ablation in the liver by ultrasound (US) is sometimes limited by thermal artefact.[6,7] These limitations may hamper the ability to assess the completeness of ablation at the tumour margin. In this study, IRE was used to ablate areas of normal porcine liver and the ability of US to measure changes in liver parenchyma at the ablation zone was investigated. The ablation zone was further examined histologically to determine the area of cellular necrosis. The study hypothesis assumed that IRE ablation causes a change in liver parenchyma that is recognizable by US and correlates with the

area of tissue necrosis. Furthermore, because the thermal effect of IRE is minimal, it was anticipated that the US artefact during the ablation process with IRE would be minimal.

Materials and methods

Three female adult pigs (each weighing 31–56 kg) were purchased from an approved supplier and preconditioned onsite. Approval was provided by the Institutional Animal Care and Use Committee at Ethicon Endo-Surgery, Inc. (Cincinnati, OH, USA). Animals received proper care and nutrition and were fasted 12 h prior to operation. Anaesthesia was induced using intramuscular telazol at a dose of 6 mg/kg and maintained with isofluorane after oral intubation. Animals were placed in the supine position and the torso hair clipped. Sterile preparation with chlorhexidine was applied in two of the three study animals. One animal was maintained under anaesthesia for 6 h after all ablations were performed and was then killed using a lethal injection of potassium chloride. The other two animals were recovered after ablations and submitted to repeat general anaesthesia 24 h later, after which they were killed with potassium chloride injection.

All animals underwent midline laparotomy. Two needle electrodes were placed directly into the liver parenchyma at the desired locations with the aim of placing the electrodes 1.5 cm apart. There were no specific targets within the normal porcine livers, but ablations were varied between the right and left lobes and segments. The current IRE platform produces the most consistent results when probes are placed 1.5 cm apart and thus attempts were made to keep this distance uniform. The normal porcine livers used were on average <4–5 cm thick in most segments, and thus probes were located 1–3 cm deep in the liver parenchyma. The placement of electrodes was guided using US. The IRE voltage fields were created by a generator applying 3000-V, 10-microsecond pulses of direct current between needle electrodes. Pulses were applied in bursts of 10 pulses and six to 15 bursts (60–150 pulses) were applied per ablation. The ablation zone was measured by US intraoperatively after the procedure and again at the time of organ harvest immediately after the animal had been killed, at either 6 h or 24 h after ablation. Diameters were measured and reported in millimetres at the area of maximum ablation effect as estimated by US (±1 standard deviation). Surface area was reported in square centimetres and calculated using the formula for obtaining the area of an ellipse (area = $a \times b \times \pi/10$, where a and b are the radii along the long and short axes in millimeters, respectively). Volume was reported in cubic centimetres and calculated using the formula for obtaining the volume of an ellipsoid [volume = $(4/3) \times pi \times a \times b \times c/10$, where a and b are the radii along the long and short axes, respectively, and c is half the length of the ellipsoid estimated by US in millimeters].

When the animals had been killed, whole livers were harvested. Livers were sectioned approximately every 1–2 cm and representative samples were frozen or fixed in formalin. Ablation zones were photographed and measured. Formalin-fixed tissues were sectioned and stained with haematoxylin and eosin and evaluated microscopically by an independent pathologist (Vet Path Services, Inc., Mason, OH, USA) for changes in morphology and overall tissue reaction to IRE. Frozen tissue samples were stained with nitroblue tetrazolium and the percentage of cell death within areas of interest was determined by histomorphometry using Image Pro Plus Version 6.3 (Media Cybernetics, Inc., Silver Spring, MD, USA).

Results

A total of 22 ablations were undertaken in three adult female pig livers using IRE during laparotomy. The median distance between the two probes measured by US just prior to firing was 1.5 cm (range: 0.95–1.70 cm). During the process of IRE ablation, hyperechoic changes consistent with minimal thermal energy were typically visible. A visible change in the hepatic parenchyma was detectable by US after each ablation and was confirmed by a palpable change from soft to firm hepatic parenchyma at each location. No immediate complications occurred during IRE ablation, and about half of the ablations were associated with mild muscle contractions. None of the ablations overlapped in any animal.

The median time from IRE ablation to assessment of parenchymal change by US was 20 min (range: 9–55 min). The mean maximum diameter of the ablation zone measured by US intraoperatively was 20.1 ± 2.7 mm. The mean cross-sectional area of ablation measured by US was 20.5 cm^2 and the mean volume of ablation was 110.9 cm^3. One animal was killed approximately 6 h after IRE ablations had been completed and two animals were killed 24 h after ablations had been completed. The mean maximum diameter of the ablation zone measured by US at the time of organ harvest was 20.4 ± 2.4 mm. The mean cross-sectional area of ablation measured by US at organ harvest was 18.4 cm^2. The mean volume of ablation at organ harvest was 142.7 cm^3.

The length of the long axis and surface area of the ablation zone were estimated by US using various US functions, including free-hand measurements of the long and short axes, the drawing of an ellipse around the ablation zone and the eSIEcalc function, which estimates the ablation zone (Siemens S200 ultrasound, system software version VA15(X), Siemens Corp., Washington, DC, USA) (Fig. 1). All three modalities made comparable estimates of the ablation zone long axis when measured soon after IRE ablation or at the time of organ harvest (Fig. 2). Gross measurements of the ablation zone were also made after histopathologic staining (Fig. 3a). The mean diameter of the zone of necrosis obtained by histologic staining was 20.3 ± 2.9 mm, and the mean cross-sectional area was 21.0 cm^2. Mean measurements of the long and short axes and the surface area of necrosis as measured by histologic stain did not differ between the liver harvested at 6 h after ablation and the two livers harvested at 24 h after ablation (data not shown). All measurement data are summarized in Table 1.

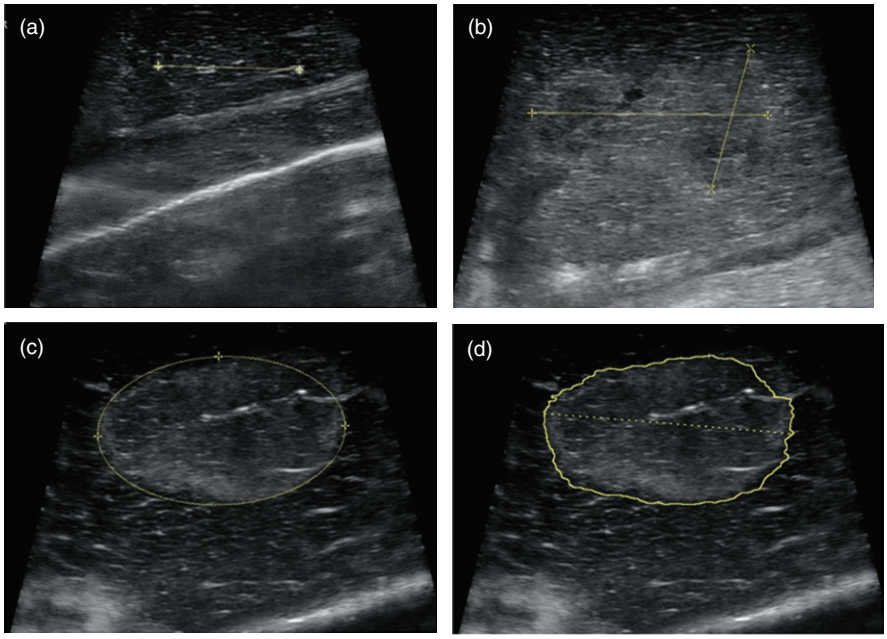

Figure 1 (a) Needle probes are placed into the liver under ultrasound guidance with the goal of placing the probes 1.5 cm apart. (b) After irreversible electroporation (IRE), the long and short axes of the zone of ablation are measured freehand. (c) After IRE, the zone of ablation is measured using an ellipse. (d) After IRE, the zone of ablation is measured using the eSIEcalc function (Siemens Corp.)

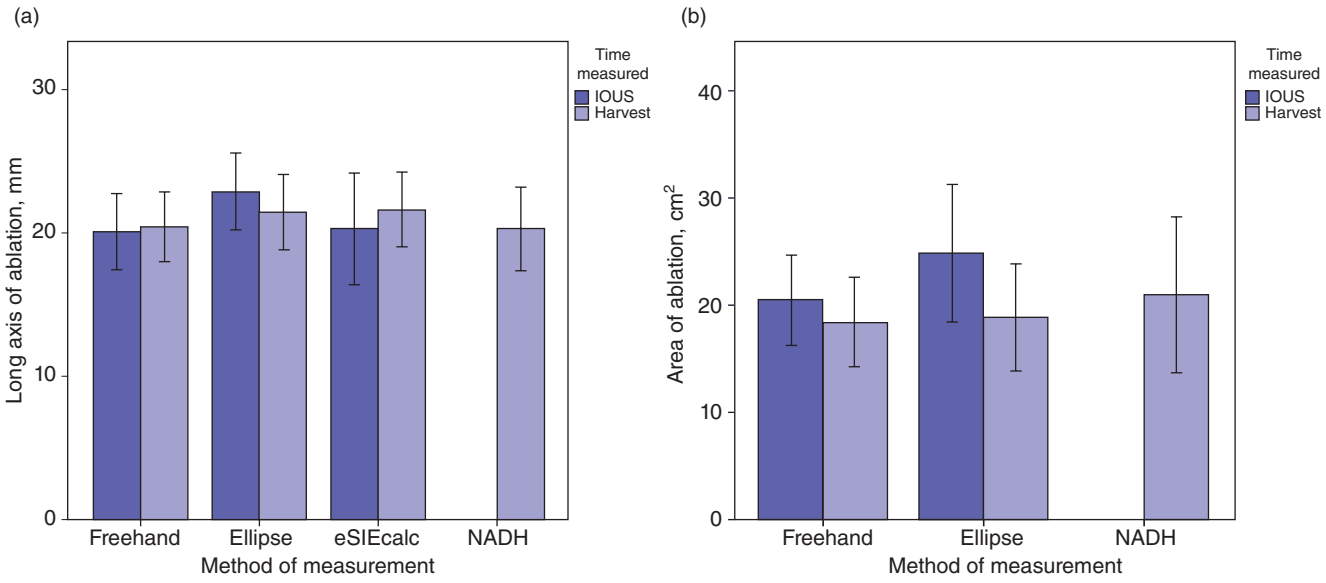

Figure 2 (a) Comparison of measurements of the long axis of the ablation zone (mm) estimated using three different ultrasound methods and histologic analysis [NADH (nicotinamide adenine dinucleotide hydride)]. (b) Comparison of measurements of the cross-sectional area of ablation estimated using two different ultrasound methods and histologic analysis. Error bars represent ±1 standard deviation. IOUS, intraoperative ultrasound

Histopathologic examination of tissue samples revealed changes consistent with hepatocellular necrosis at ablation sites. At 6 h after ablation, the ablated zones were non-encapsulated and irregular, and were surrounded by viable liver tissue within the affected region. Lytic necrosis was observed at the centre of some ablated zones, with mild to marked coagulative necrosis mixed with inflammatory cell infiltration and haemorrhage. Vascular fibrinoid necrosis, mineralization/calcification and throm-

bosis of blood vessels were also seen within the ablated areas. The mean percentage of dead cells within areas of interest at 6 h was 77.0% (range: 50.1–95.7%). Findings were similar at 24 h after ablation, when zones of ablation were characterized again by mild lytic necrosis in the centre of some ablation zones and moderate coagulative necrosis associated with haemorrhage and mixed cell infiltration. The mean percentage of dead cells within areas of interest at 24 h was 98.3% (range: 95.5–99.4%). The architecture of endothelial cell-lined structures within the middle of ablation zones was generally preserved (Fig. 3b). In ablation zones nearer to larger intraheptic portal pedicle or hepatic venous branches, smooth muscle cell necrosis was identified, but structure and blood or bile flow were seen to be preserved on US.

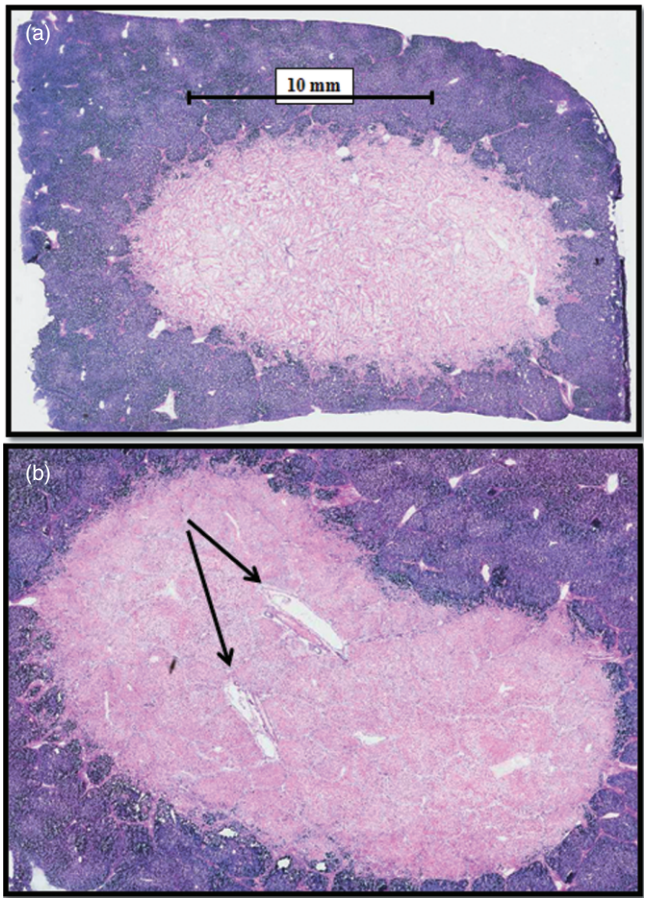

Figure 3 (a) Histologic examination after irreversible electroporation in normal porcine liver reveals near complete cellular necrosis in the ablation zone (pink). (b) Within the ablation zone, the architecture of endothelial cell-lined structures is preserved (arrows)

Discussion

This study demonstrates that a visible change in normal porcine liver parenchyma detected by US within minutes of IRE is consistent with the area of eventual cellular necrosis. Furthermore, the zone of ablation at 24 h shows nearly 100% necrosis by histologic analysis. It is feasible that the repopulation of the tissue scaffold with live cells may account for the few live cells that were found. Measuring the zone of ablation in real time during the process of solid tumour ablation, either with thermal technologies or with IRE, is critical to determining whether the zone has covered an area sufficient to result in total tumour cell kill. Although the use of US to measure a zone of thermal ablation applied using radiofrequency or microwave energy may be limited by thermal artefact, no such artefacts impairing the ability to measure the IRE ablation zone with US were encountered in this study.

As in the present study, Rubinsky and colleagues found the zone of ablation made by IRE in a porcine liver model to correlate well with the zone of cellular necrosis.[8] Furthermore, and similarly to results in this study, the architecture of endothelial cell-lined structures (blood vessels and bile ducts) seems to be preserved even when the structures are included in the IRE ablation zone.[4] A study using a rat model has shown that full recovery after endothelial cell necrosis in IRE is possible because the extracellular structures are preserved.[9] In a study by Lee *et al.*, immunohistologic staining confirmed the mechanism of cell death in a porcine liver after the application of IRE is apoptosis.[10] The ability of IRE to induce apoptosis and necrosis in cancer cells has been demonstrated in many preclinical studies, including in the prostate[11] and liver.[12] In addition to its use in large-animal liver models, such as that in the current study, IRE has also been used for ablation in a

Table 1 Measurements by ultrasound and histology after irreversible electroporation in normal porcine liver

Ablation zone	Measurement by IOUS	Measurement by HAR-US	Measurement by histopathology
Diameter, mm, mean ± SD	20.1 ± 2.7	20.4 ± 2.4	20.3 ± 2.9
Area, cm^2, mean	20.5	18.4	21.0
Volume, cm^3, mean	110.9	142.7	
Diameter by ellipse, mm, mean ± SD	22.9 ± 2.7	21.5 ± 2.6	
Area by ellipse, cm^2, mean	24.8	18.8	
Diameter by eSIEcalc, mm, mean ± SD	20.3 ± 3.9	21.7 ± 2.6	

IOUS, intraoperative ultrasound; HAR-US, ultrasound at the time of organ harvest; SD, standard deviation; eSIEcalc, 'Easy calc' ultrasound measurement function (Siemens Corp.).

canine brain surgery model,[13] a porcine epicardial model[14] and in normal porcine pancreas tissue.[15]

There are several limitations to the experiments presented in this study. Firstly, the setting used on the IRE generator was not varied significantly and therefore only a narrow range of IRE capability was studied. Other experiments by the current authors have shown that higher generator settings lead to a combined IRE and thermal ablation effect, but the present experiments were designed to facilitate the study of ablations created using pure IRE. It will be important in future animal experiments to vary the IRE generator settings in order to facilitate better understanding of the variability of effects and range of ablation zones. The porcine livers used in the current study were all normal and of similar size. Future studies should also determine which IRE generator settings are best in different liver tissue types, particularly in liver fibrosis and cirrhosis, and for various tumour types. Indeed, such experiments are ongoing at this time. The median time between IRE ablation and measurement by US in the present experiments was 20 min, but this delay would represent a major limitation in a clinical setting. Fortunately, the IRE effect is typically visible by US within 5 min and the slower pace used in the present study reflects the study's experimental design rather than any necessity to wait for the IRE effect to become visible. Finally, these experiments were performed using laparotomy, whereas the majority of thermal ablations are performed using laparoscopic or percutaneous techniques, and thus use of the latter techniques will be important in future studies.

Ultrasound is a common imaging modality used to guide the thermal ablation of hepatic malignancies during laparoscopic or open procedures in an operating room. Thus, it is important that US is able to measure the approximate area of ablation in any new technique, such as IRE. This study confirms the accuracy of US measurement in comparison with histopathology. It is also possible to guide thermal ablation using computed tomography (CT) or magnetic resonance imaging (MRI) and these modalities are commonly applied when such procedures are performed using a percutaneous approach, typically in an interventional radiology suite. Both CT and MRI have also been shown to image the effects of IRE in solid organs very well.[16] Therefore, the effect of IRE is measurable both by US and cross-sectional imaging modalities. There is a delay of several minutes before the IRE ablation zone is visible by US; however, this may not ultimately represent a practical limitation. Because all ablation technologies generally create predictable zones of cellular necrosis, measuring the zone of IRE or thermal ablation by US may be less important than using US to ensure that probes are placed as accurately as possible within or near the tumour. Irreversible electroporation deserves further evaluation for use in solid organ tumours, particularly in tumours that are not amenable to surgical removal or thermal ablation.

Conflicts of interest

CRS has received compensation from Ethicon-Endo Surgery, Inc. as a consultant and is a member of an external advisory board for the same company.

References

1. Edd JF, Horowitz L, Davalos RV, Mir LM, Rubinsky B. (2006) *In vivo* results of a new focal tissue ablation technique: irreversible electroporation. *IEEE Trans Biomed Eng* 53:1409–1415.
2. Davalos RV, Mir IL, Rubinsky B. (2005) Tissue ablation with irreversible electroporation. *Ann Biomed Eng* 33:223–231.
3. Kanduser M, Sentjurc M, Miklavcic D. (2006) Cell membrane fluidity related to electroporation and resealing. *Eur Biophys J* 35:196–204.
4. Charpentier KP, Wolf F, Noble L, Winn B, Resnick M, Dupuy DE. (2011) Irreversible electroporation of the liver and liver hilum in swine. *HPB (Oxford)* 13:168–173.
5. Miklavcic D, Semrov D, Mekid H, Mir LM. (2000) A validated model of *in vivo* electric field distribution in tissues for electrochemotherapy and for DNA electrotransfer for gene therapy. *Biochim Biophys Acta* 1523:73–83.
6. Garrean S, Hering J, Saied A, Hoopes PJ, Helton WS, Ryan TP *et al*. (2009) Ultrasound monitoring of a novel microwave ablation (MWA) device in porcine liver: lessons learned and phenomena observed on ablative effects near major intrahepatic vessels. *J Gastrointest Surg* 13:334–340.
7. Topp SA, McClurken M, Lipson D, Upadhya GA, Ritter JH, Linehan D *et al*. (2004) Saline-linked surface radiofrequency ablation: factors affecting steam popping and depth of injury in the pig liver. *Ann Surg* 239:518–527.
8. Rubinsky B, Onik G, Mikus P. (2007) Irreversible electroporation: a new ablation modality – clinical implications. *Technol Cancer Res Treat* 6:37–48.
9. Maor E, Ivorra A, Rubinsky B. (2009) Non-thermal irreversible electroporation: novel technology for vascular smooth muscle cells ablation. *PLoS ONE* 4:e4757.
10. Lee EW, Loh CT, Kee ST. (2007) Imaging guided percutaneous irreversible electroporation: ultrasound and immunohistological correlation. *Technol Cancer Res Treat* 6:287–294.
11. Rubinsky J, Onik G, Mikus P, Rubinsky B. (2008) Optimal parameters for the destruction of prostate cancer using irreversible electroporation. *J Urol* 180:2668–2674.
12. Miller L, Leor J, Rubinsky B. (2005) Cancer cells ablation with irreversible electroporation. *Technol Cancer Res Treat* 4:699–705.
13. Garcia PA, Rossmeisl JH Jr, Robertson J, Ellis TL, Davalos RV. (2009) Pilot study of irreversible electroporation for intracranial surgery. *Conf Proc IEEE Eng Med Biol Soc* 2009:6513–6516.
14. Lavee J, Onik G, Mikus P, Rubinsky B. (2007) A novel non-thermal energy source for surgical epicardial atrial ablation: irreversible electroporation. *Heart Surg Forum* 10:162–167.
15. Charpentier KP, Wolf F, Noble L, Winn B, Resnick M, Dupuy DE. (2010) Irreversible electroporation of the pancreas in swine: a pilot study. *HPB (Oxford)* 12:348–351.
16. Lee EW, Chen C, Prieto VE, Dry SM, Loh CT, Kee ST. (2010) Advanced hepatic ablation technique for creating complete cell death: irreversible electroporation. *Radiology* 255:426–433.